

Mechanical properties of resin composite reinforced with synthesized nano-structured hydroxyapatite

Lamiaa M. Moharam^{1*}, Marwa. A. Sherief², Shaymaa M. Nagi¹

¹Restorative and Dental Materials Research department, National Research Centre, Giza. Egypt.

²Inorganic chemistry department, National Research centre, Giza. Egypt.

Abstract : This study aimed to prepare nanostructured hydroxyapatite (nHAp) by sol-gel method and assess the influence of its incorporation with different concentrations into a dental resin composite. The prepared nHAp powder was characterized by X-ray diffraction (XRD), infrared spectrum (IR), and scanning electron microscopy (SEM). nHAp was added to a commercial dental resin composite at four different concentrations (0, 1.5, 2, and 5 wt%). Nanostructured HAp incorporated dental resin composites were tested for their micro-hardness (VHN), degree of monomer conversion (DC), flexural strength (FS). The data were analyzed using one-way ANOVA and Tukey's post hoc test ($P \leq 0.05$). The results of characterization indicated that; HAp formed in small particles with aggregates have the particles <80 nm. The incorporation of 2 wt% nHAP revealed statistically significant highest mean micro-hardness values (104 ± 1.7), and flexural strength (203.6 ± 27.3 MPa), compared to other nHAp concentrations. The incorporation of nHAp did not influence the degree of monomer conversion, which was higher than 50% with 20 seconds of photo-polymerization for all tested groups. The analysis of results showed that the incorporation of 2 wt% of nanostructured hydroxyapatite into a dental resin composite had positively influenced the mechanical properties. Also, the inclusion of nanostructured hydroxyapatite increased the tested mechanical properties of the dental resin composite and might be promising filler for dental resin composites.

Keywords: hydroxyapatite synthesis; mechanical properties, resin composite.

Introduction

Hydroxyapatite (HAp) is the major biomineral component found in human hard tissues (teeth and bone). It is has the formula $\{Ca_2(PO_4)_3(OH)\}$. It is the major mineral part of the tooth enamel, and it composes more than 60 wt% of tooth dentin.^{1,2}

Synthetic hydroxyapatite has been widely introduced into the field of dentistry as a biomaterial due to its similarity in crystallography and chemical composition to that of human hard tissue.³

It has high biocompatibility and bioactivity under *in vivo* conditions, also it has multiple applications including: bone tissue engineering; restoration of periodontal defects, fillers for reinforcing dental restorations^{4,5} and adhesives⁶, post-bleaching desensitizing agent⁷, early carious lesions treatment⁸⁻¹⁰ and as a remineralizing agent for teeth in toothpastes¹¹.

Resin composites are extremely important in the field of dentistry especially as direct aesthetic restorations. Manufacturers are constantly trying their best to improve and enhance their mechanical properties to withstand the heavy occlusal forces during mastication. Several inorganic and organic fillers were planned to increase the dental composite resin mechanical as well as optical properties. The use of HAp as a filler in dental resin composites seems to be successful. As HAp is the structural prototype for the principle inorganic crystalline composition of the tooth. Moreover; HAp is radio-opaque, resistant to moisture and possesses the ideal hardness as all other dental resin composite filler particles¹²

There are many techniques for preparation of HAp such as sol-gel synthesis, solid-state reactions, chemical precipitation, spray pyrolysis, combustion synthesis, micro-emulsion and microwave synthesis.^{13,14}

The sol-gel technique is the common method used to obtain nano-sized HAp of high purity¹⁴⁻¹⁷.

It is believed that nHAp with grain size <100 nm in at least one direction has a high surface activity and ultrafine structure similar to the mineral found in the tooth hard tissues.¹⁸

The degree of conversion (DC) of the resin composite (methacrylate monomer bonds) is the degree to which carbon-carbon double bonds is converted into carbon-carbon single bonds giving rise to polymer chains.[19] Fourier transformation infrared spectroscopy (FT-IR) is the most reliable direct method to detect the degree of monomer conversion for resin composites which influences their mechanical properties such as flexural strength, wear resistance and surface hardness.¹⁹

With the market floating with new dental resin composites claiming their superior mechanical properties this study was conducted to synthesize nano-structured hydroxyapatite using sol-gel method, and evaluate its crystalline structure, morphology and elemental composition. Moreover; it was conducted to investigate the influence of its incorporation into a commercially available dental resin composite with different concentrations on the surface micro-hardness, degree of monomer conversion and flexural strength.

2. Materials and method

2.1. Materials

One commercially available nano-hybrid dental resin composite was tested in this study. The material manufacturer, composition and batch number were listed in (Table 1).

Table 1. Material description, manufacturer, composition and batch number.

Material	Composition	Manufacturer	Batch number
Filtek® Z250 XT Nano-Hybrid Universal Restorative Resin composite	55-65 wt% Water. 30-40 wt% Phosphoric Acid. 5-10 wt% Synthetic Amorphous Silica. Surface Modified Zirconia/Silica (0.1-10 microns). 20 nm Surface Modified Silica Particles. 81.8 wt% Inorganic Filler (67.8 vol%). Bis-GMA, UDMA, Bis-EMA, PEGDMA, TEGDMA	3M ESPE Dental Products 3M Center, St. Paul, MN 55144-1000, USA	N 495009 N 504756
Bis-GMA: Bis-Phenol-A glycidyl-methacrylate. Bis-EMA: Ethoxylated bisphenol A dimethacrylate. UDMA: Urethane dimethacrylate. PEGDMA: Poly (ethylene glycol) dimethacrylate. TEGDMA: Triethylene glycol dimethacrylat.			

Synthesized hydroxyapatite powder (HAp) was used in the study in four different concentrations 0 wt%, 1.5 wt%, 2 wt% and 5 wt%.

2.2.Preparation of HAp by sol-gel method

A solution of 0.25 M di-ammonium hydrogen phosphate $[(\text{NH}_4)_2 \text{HPO}_4]$ was prepared in distilled water (3.3 g /100 ml) and it was presented as solution-1. Ammonium hydroxide $[\text{NH}_4 \text{OH}]$ was added to the prepared solution to adjust the pH to be 10. Another solution of 1.0 M calcium nitrate tetra-hydrate $[\text{Ca} (\text{NO}_3)_2 \cdot 4\text{H}_2\text{O}]$ was prepared in distilled water (23.615 g /100 ml) and it was presented as solution-2, which was slowly added into solution-1. The mix was kept stirred for 4 hours at 65 °C. A white gel was produced as a result of the reaction. The white gel was kept in room temperature for 24 hours, and then dried in an oven for 20 hours at 85 °C. A dried white powder was obtained.²⁰

3.Characterization

3.1.X-ray diffraction (XRD) analysis

Power X-ray diffraction (XRD) was performed on Bruker D8 advance diffractometer (Germany) using $\text{CuK}\alpha$ radiation (1.54 Å) and a Ni filter.

3.2.Infrared Spectrum (IR)

Fourier Transformer Infrared Spectrometer (Nexus 670 FTIR, USA) was used to obtain Infrared absorption spectra (IR) using Potassium Bromide (KBr) pellet technique at a wavelength range from 400 to 4000 cm^{-1} .²¹

3.3.Scanning electron microscopy (SEM)

The surfaces of prepared specimens were gold sputtered to reveal the surface morphology using SEM (JEOL, JSM-t20)²² at 4000 X magnification.

4.Mechanical properties testing

4.1.Study design and specimen grouping

One hundred and thirty specimens were prepared and equally divided into 13 groups (n=10/group) according to the four HAp concentrations (0 wt%, 1.5 wt%, 2 wt% and 5 wt %) investigated in the study. Forty of those specimens were subjected to the micro-hardness test while another 40 specimens were tested for flexural strength and finally 50 specimens were tested for the degree of monomer conversion test.

4.2.Hydroxyapatite-resin composite reinforced specimen preparation

The prepared HAp powder particles were incorporated into the uncured resin composite (Filtek™ Z250 XT) in four different concentrations (0 wt%, 1.5 wt%, 2 wt% and 5 wt%). Both HAp powder particles and the uncured dental resin composite were mixed thoroughly on a glass slab over wide area using a gold-plated spatula. Thorough and consistent mixing was done under safe-light conditions in order to prevent ambient light from polymerizing the uncured dental resin composite during mixing. The mixing procedure was continued until all the HAp powder particles were fully incorporated into the uncured dental resin composite till homogenous, workable and plastic resin composite consistencies were finally obtained.

4.3.Specimen preparation

One Light Emitting Diode light-curing unit (LED, Elipar S10, 3M ESPE; USA) with light intensity output of 1000 mW/cm^2 was used to photo-polymerize the specimens throughout the whole study. The light intensity output of the light curing unit was determined using a Demetron radiometer (Model 100, Demetron Research Corporation, Danbury, CT, USA).[23] The diameter of the light-curing guidance tip was 6 mm as measured using a digital caliper (Mitutoyo, Tokyo, Japan).²⁴

4.4.Micro-hardness testing

Split Teflon moulds of 4 mm diameter and 2 mm thicknesses, encircled with a copper ring for stabilization, were used to prepare the cylindrical specimens. The moulds were first mounted on the top of a microscope slide and a Mylar strip, and then the moulds were filled in one increment with one of the four-

concentration HAp reinforced dental resin composite. The top side of the mould was covered with a second Mylar strip to prevent the formation of the oxygen inhibited layer at the dental resin composite top surface. A glass slide and 1 kg load were applied for 30 seconds to ensure consistent packing of the specimens, after which the load and the glass slide were removed.²⁵

The top surface of each prepared specimen was light-cured for 20 seconds as recommended by manufacturer. The light-curing guidance tip was kept centered and in direct contact with the second Mylar strip. After photo-polymerization, the cylindrical specimens were removed from the Teflon moulds and the excess dental resin composite material was removed using a sharp scalpel.²⁶

The top surfaces of the specimens were identified with an indelible mark. The specimens were stored dry in tightly sealed, light-proof containers before the micro-hardness test was conducted, in complete darkness at 37 °C for 24 hours.¹⁹

A total of 40 specimens were tested for their micro-hardness using Vickers micro-hardness tester (Nexus 4503, INNOVATEST, Netherlands, Europe). Three randomized indentations on the top surface of each specimen were made with 500 g load and a dwell time of 15 seconds.^{27,28}

For randomization, specimens were arbitrarily rotated before indentations. Calculations were made using computer software (Hardness-Course Vickers/ Brinell/ Rockwell copy right IBS 2012 version 10.4.4).

4.5. Flexural strength testing

Rectangular dental resin composite specimens for the flexural strength test were fabricated in custom-made split Teflon moulds which were encircled with a copper ring for stabilization according to ISO 4049 specifications, except for the dimensions of each specimen which were: 12 mm in length, 2 mm in width, and 2 mm in height.^{29,30}

The prepared specimens were packed into the moulds, which was located on top of a Mylar strip placed over a thick glass slab. The top surfaces of the specimens were covered with another Mylar strip to prevent oxygen inhibited layer formation at the resin composite top surface. A glass slide and 1 kg load were applied on each specimen top surface to ensure consistent packing of the specimens for 30 seconds after which the load and the glass slide were removed.²⁵

The prepared specimen length (12 mm) was double the diameter of the light curing tip used in the study (6 mm), so that, each half of the prepared specimens were light-cured for 20 seconds as recommended by manufacturers.²³

After photo-polymerization, the specimens were removed from the mould, excess composite flashes were removed using sharp scalpel and then stored in distilled water, and in tightly sealed containers at 37 °C for 24 hours before the flexural strength testing was conducted. Ten specimens were prepared for each group (n=10); in total, 40 specimens were individually and horizontally mounted in a custom made fixture (three point bend test assembly; two parallel stainless steel rods with span length of 12 mm for supporting the specimen, with the damage site centrally located on the tensile side) on a computer controlled materials testing machine (Model LRX-plus; Lloyd Instruments Ltd., Fareham, UK) with a load cell of 5 kN and data were recorded using computer software (Nexygen-MT; Lloyd Instruments). Specimens were statically compression loaded until fracture at a crosshead speed of 1 mm/min. The flexural strength (σ_s) of each specimen was calculated in Mega Pascal (MPa) according to the following equation:

$$\sigma_s = 3LF / 2BH^2 \quad (1)$$

(Where, **F**: is the maximum load in Newton, **L**: is the distance in mm between the supports, **B**: is the width in mm of the specimen and **H**: is the height of the specimen in mm).

4.6. Degree of monomer conversion testing

Sectional Teflon moulds of 4 mm diameter and 2 mm thicknesses encircled with a copper ring for stabilization, were used to prepare the specimens. The moulds were mounted on the top of a microscope slide and a Mylar strip, and then each mould was filled in bulk with one of the four-concentration HAp-incorporated

dental resin composite. The top side of the mould was covered with a second Mylar strip to prevent the formation of the oxygen inhibited layer at the resin composite top surface. A glass slide with a load of 1 kg was applied for 30 seconds to ensure consistent packing of the specimens, after which the load and the glass slide were removed.²⁵

Specimens were photo-polymerized from the top surface only for 20 seconds as recommended by the manufacturer. The light-curing tip was kept centered and in direct contact with the second Mylar strips.²³

The specimens were stored dry in light-proof containers and in complete darkness at 37 °C for 24 hours before the FT-IR analysis was conducted to prevent ambient light from causing additional post light-curing polymerization.²⁶

Forty specimens were tested for their degree of monomer conversion using (Jasco FT-IR 6400, Japan). FT-IR spectra of the uncured and cured resin composite materials were obtained using 24 scans at 4 cm⁻¹ in the absorbance mode and wavelength ranging from 400-4000 cm⁻¹. The FT-IR spectroscopy was completed using Potassium Bromide (KBr) pellet technique. An additional 10 uncured specimens (un-polymerized) were prepared for FT-IR testing to be used as control specimens. For the control specimens; 2 mg of each of the uncured dental resin composite (0 wt% HAp), were blended with 7 mg of Ispectropic grade (IR) Potassium Bromide powder (KBr) in a specimen holder; then it was pressed into a transparent pellet (1 mm thickness) under heavy pressure for one minute, using a pellet maker kit (KBr Product-A-Press, International Crystal Labs, Garfield, NJ, USA), before it was subjected to FT-IR analysis.^{19,31}

Each light-cured (polymerized) prepared specimen was completely crushed and ground into a fine powder using a mortar and a pestle. Subsequently, 2 mg of the each of the resin composite powder were blended with 7 mg of Ispectropic grade (IR) Potassium Bromide in a specimen holder, and then it was pressed into a transparent pellet using a pellet maker kit.¹⁹

The specimen holder was transferred to the spectrometer and a spectrum was obtained using the same parameters as for the uncured dental resin composite specimens. FT-IR spectra of the photo-polymerized dental resin composites specimens were obtained after 24 hours in dark storage at 37 °C.¹⁹

The DC was calculated from the ratio between the absorbance peaks of the aliphatic C=C bond (1638 cm⁻¹) to the aromatic C=C (1608 cm⁻¹), used as an internal standard, obtained from the polymerized and unpolymerized specimens by the following equation:³²

$$DC\% = 100 \times [1 - (R_{\text{polymerized}} / R_{\text{unpolymerized}})] \quad (2)$$

(Where, **R**= peak at 1638 cm⁻¹/ peak at 1608 cm⁻¹).

4.7. Statistical analysis

Data were presented as mean, standard deviation (SD) and standard error (SE) values. Data were explored for normality using D'Agostino-Pearson test for Normal distribution. Degree of monomer conversion, Micro-hardness and Flexural strength showed a normal distribution. One way-ANOVA has been used to study the effect of Nano-hydroxyapatite concentrations. Tukey's post-hoc test was used for pair-wise comparison between the means when ANOVA test was significant. Statistical analysis was performed with IBM® SPSS® (SPSS Inc., IBM Corporation, NY, USA) Statistics Version 22 for Windows.

5. Results

5.1. HAp characterization results

(Figure 1) represented the x-ray diffraction pattern of the prepared HAp specimens.

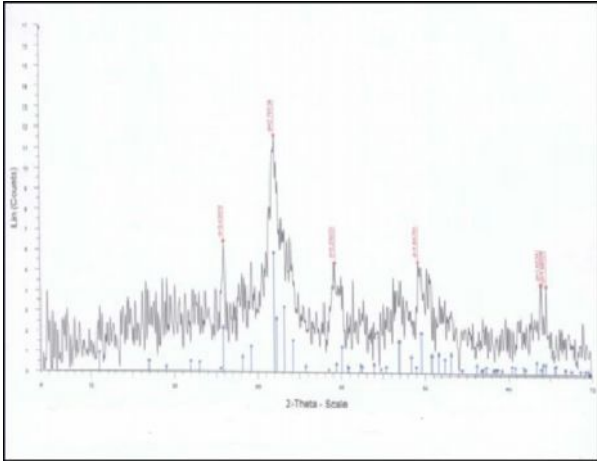


Figure 1. XRD patterns of prepared HAp specimens.

The main characteristic peaks of HAp were shown especially at $2\theta = 33$ (JCPDS 86-0740). The estimated particles size of the prepared powder showed that its particles have diameter < 80 nm in range.

(Figure 2) represented the IR spectra of the prepared HAp specimen. The IR chart showed that a broad band at ~ 3425.3 - 3440 cm^{-1} was formed. Also, a strong band appeared at 1000 - 1100 cm^{-1} beside another weak one at ~ 930 cm^{-1} . Two other sharp bands at ~ 580 and 558 cm^{-1} were formed. A sharp band appeared at ~ 1420 cm^{-1} . The appearance of these bands emphasized the formation of hydroxyapatite.

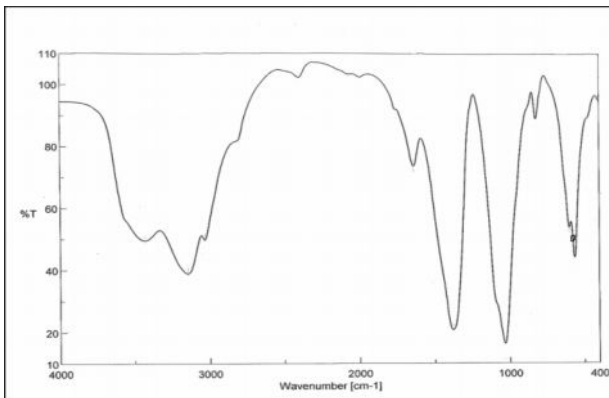


Figure 2. FTIR spectra for the prepared HAp specimens.

(Figure 3) Showed SEM photographs for the prepared HAp specimens. The photographs of the powder showed the formation of agglomerated forms with very fine pores.²²

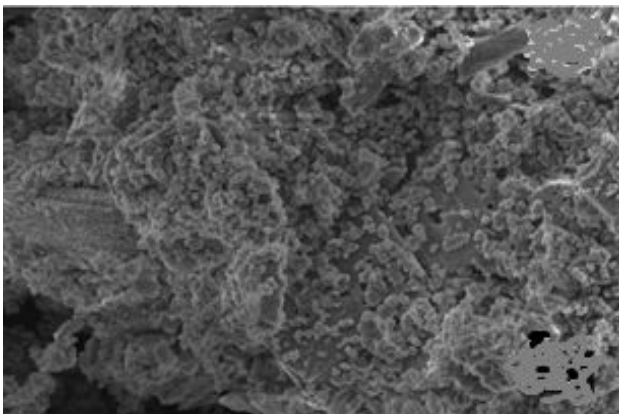


Figure 3. SEM microphotograph for the prepared HAp specimens.

5.2. Mechanical properties results

Means and standard deviations (SD) for different tested parameters for different nano-hydroxyapatite concentrations were presented in (Table 2).

Regarding the micro-hardness mean values, the 2 wt% HAp group revealed the highest mean statistically significant micro-hardness values (104 ± 1.7), followed by 0 wt% HAp group (93.2 ± 2.06), 1.5 wt% HAp group (92.5 ± 4.3), and finally the lowest mean values which were recorded for the 5 wt% HAp group (90.9 ± 2.2), where there was no statistically significant difference between them.

On the other hand, for the flexural strength mean values in MPa, 2 wt% HAp group revealed the highest mean statistically significant values (203.6 ± 27.3), followed by 0 wt% HAp group (132.6 ± 16.07) and 1.5 wt% HAp group (101.8 ± 17.08), where there was no statistically significant difference between them.

5 wt% HAp group showed the least statistically significant mean flexural strength values (65.7 ± 16.2), that was insignificantly different from the 1.5 wt% HAp group mean values.

All groups showed a degree of monomer conversion higher than 50 % with 20 seconds of photopolymerization. There were no statistically significant differences between the experimental groups (1.5, 2 and 5 wt% HAp) and the control group (0 wt% HAp).

The highest mean degree of monomer conversion value was 73.8 % and it was recorded by the 2 wt% HAp group.

Table 2. Means and standard deviations (SD) for different tested parameters for different Nano-hydroxyapatite concentrations.

	Nano-hydroxyapatite concentrations								p-value
	0 wt%		1.5 wt%		2 wt%		5 wt%		
	Mean	SD	Mean	SD	Mean	SD	Mean	SD	
Micro-hardness	93.24 ^b	2.06	92.57 ^b	4.37	104.00 ^a	1.73	90.97 ^b	2.22	0.002*
Degree of monomer conversion (%)	73.15	0.96	70.53	1.67	73.85	4.18	67.94	5.30	0.230 NS
Flexural strength (MPa)	132.67 ^b	16.07	101.80 ^{bc}	17.08	203.67 ^a	27.30	65.70 ^c	16.21	$\leq 0.001^*$

*Significant at $p \leq 0.05$, N =Number

Pearson correlation between the degree of monomer conversion, surface micro-hardness and flexural strength, was presented in (Table 3). There was an insignificant correlation between degree of monomer conversion and micro-hardness, $r = 0.304$, p (2-tailed) = 0.337. There was a significant positive correlation between degree of monomer conversion and Flexural strength, $r = 0.578$, p (2-tailed) = 0.049. There was a significant positive correlation between micro-hardness and mean Flexural strength, $r = 0.837$, p (2-tailed) = 0.001.

Table 3. Results of Pearson Correlation for the correlation between degree of monomer conversion (%), mean micro-hardness and Flexural strength (MPa).

		Micro-hardness	Degree of monomer conversion (%)	Flexural strength (MPa)
Micro-hardness	Pearson Correlation	1	0.304	0.837
	Sig. (2-tailed)		0.337 NS	0.001*
	N	12	12	12
Degree of monomer conversion (%)	Pearson Correlation	0.304	1	0.578
	Sig. (2-tailed)	0.337 NS		0.049*
	N	12	12	12
Flexural strength (MPa)	Pearson Correlation	0.837	0.578	1
	Sig. (2-tailed)	0.001*	0.049*	
	N	12	12	12

*Significant at $p \leq 0.05$, N = Number.

6. Discussion

In the current study, a nano-structured hydroxyapatite was successfully prepared using a sol-gel process. At the nano-scale, the hydroxyapatite particles size (<80 nm) could be observed with a small aggregates.^{20,21}

In the infrared Spectrum the band at $\sim 3425.3-3440 \text{ cm}^{-1}$ was attributed to the vibration of the hydroxyl (OH⁻) ions in the lattice as proposed.³³

On the other hand; the band at $1000-1100 \text{ cm}^{-1}$ along with a weak one at $\sim 930 \text{ cm}^{-1}$ were due to the stretching vibrations of phosphate (PO₄⁻³) ions. The bands at ~ 580 and 558 cm^{-1} were due to the deformation vibrations of the phosphate ions (PO₄⁻³).³⁴

The band at $\sim 1420 \text{ cm}^{-1}$ was corresponding to carbonate ions (CO₃⁻²) incorporated with hydroxyl ions (OH⁻) sites on the surface of the hydroxyl apatite that might be due to the atmospheric carbon dioxide (CO₂).³⁵

Regarding the SEM microphotography of the prepared HAp specimens, the present fine pores might be an advantage especially when it is used for biomedical purposes.³⁶

Moreover; the particle sizes did not exceed 80 nm, and that was in conformity with the XRD findings. nHAp that was prepared in the current study obtained favourable results for incorporation into the dental resin composite, and the 2 wt% nHAp group showed the most favorable results.

It seemed that the mass fraction of nHAp incorporated in the dental resin composites perform a significant role in determining the mechanical properties. Results in (Table 2) indicated that incorporating small mass fraction of nHAp into the dental resins composites significantly enhanced the micro-hardness and flexural strength, when the critical mass fraction (percolation threshold) was about 2 wt%, while the mechanical properties decreased to be insignificant from the control group (0 wt% HAp), and when the nHAp was increased up to 5 wt%. The incorporation of the nHAp into BisGMA/TEGDMA matrix of the dental resin composites might have double-edged effects; the reinforcing effect due to the well distributed nHAp, and the deteriorating effect due to the development of nHAp agglomerates.

The nHAp could be evenly dispersed in the dental resin composites at a low loading rate, which results in the enhancement of the dental resins mechanical properties. As the nHAp mass fraction increased to 5 wt%, a small fraction of nHAp begin to form bundles in the dental resin matrix, which could proceed as a mechanical weak point in the dental resins and led to a great extent to decrease the mechanical properties (micro-hardness and flexural strength).

These results were in accordance with Chen *et al.*³⁷ who observed by SEM that the HAp nanofibers were uniformly distributed within the matrix at a small mass fraction (2 wt%). On the other hand when 5wt%

HAp nanofibers were incorporated in resin composite, nHAp bundles could be observed, which were responsible for decreasing the biaxial flexural strength of the tested dental resin composite, compared to 2 wt% HAp nanofibers. In addition, they revealed by their SEM microphotographs that incorporation of HAp nanofibers in dental resin composites containing silica; seemed to be easier to form larger bundles and aggregates compared to silica free resin composite, which was the case in the current study, as the dental resin composite that was used in this study was silica filled.³⁷

On the other hand, the incorporation of nHAp showed no effect on the degree of monomer conversion between the tested groups. The degree of monomer conversion of dental resin composites directly affects the mechanical properties of the resin composite.^{38,39}

Both intensity of the light source and attenuating power of the material control the degree of monomer conversion. The light intensity emit from the LED light curing unit decreases as it pass through the resin material and the depth of cure of the dental resin composite is to a great extent affected by the quantity of light that reach the photo-initiator.

It has been revealed^{40,41} that light scattering was correlated to filler particle size in the resin composites, which was maximize when the filler particle size is one half the wavelength of photo-polymerizing light, resulting in a lesser transmission coefficient and lesser depth of cure. Transmission coefficient is affected by the wavelength of photo-polymerizing light, type and amount of filler particles, and the refractive indices of both resin matrix and the fillers.

Thus as all the previously mentioned variables affecting the degree of monomer conversion of dental resin composite, were standard in this study. There was no statistically significant difference between all tested groups.^{40,41}

7. Conclusions

From the analysis of the obtained results, it could be concluded that HAp was produced using simple and smart method in nano-scales. The incorporation of 2 wt% of nano-structured hydroxyapatite into a dental resin composite restorative material was promising filler regarding the mechanical properties of the dental resin composite.

Conflict of interest

All authors of the study declare that there is not any actual or potential conflict of interest.

8. References

1. Goenka S., Balu R., Sampath K.T., Effect of nanocrystalline calcium deficient hydroxyapatite incorporation in glass ionomer cements, *J. Mech. Behav. Biomed. Mat.*, 2012, 7, 69-76.
2. Al-Sanabani J.S., Madfa A.A., Al-Sanabani F.A., Application of calcium phosphate materials in dentistry, *Int. J. Biomat.*, 2013, 2013, 1-12.
3. Ramli R., Adnan R., Bakar M., Synthesis and characterization of pure nanoporous hydroxyapatite, *J. Phys. Sci.*, 2011, 22, 25-37.
4. Arita K., Yamamoto A., Shinonaga Y., Hydroxyapatite particles characteristics influence the enhancement of the mechanical and chemical properties of conventional restorative glass ionomer cement, *Dent. Mat. J.*, 2011, 30, 672-683.
5. Zhang H., Darvell B.W., Mechanical properties of hydroxyapatite whisker-reinforced bis-GMA-based resin composites, *Dent. Mat.*, 2012, 28, 824-830.
6. Leitune V.C., Collares F.M., Trommer R.M., The addition of nanostructured hydroxyapatite to an experimental adhesive resin, *J. Dent.*, 2013, 41, 321-327.
7. Browning W.D., Cho S.D., Deschepper E.J., Effect of a nano-hydroxyapatite paste on bleaching related tooth sensitivity, *J. Esth. Rest. Dent.*, 2012, 24, 268-276.
8. Li L., Pan H., Tao J., Repair of enamel by using hydroxyapatite nanoparticles as the building blocks, *J. Mat. Chem.*, 2008, 18, 4079-4084.

9. Huang S., Gao S., Cheng L., Remineralization potential of nano-hydroxyapatite on initial enamel lesions: An in vitro study, *Car. Res.*, 2011, 45, 460-468.
10. Huang S., Gao S., Cheng L., Combined effects of nano-hydroxyapatite and Gallachinensis on remineralization of initial enamel lesion in vitro, *J. Dent.*, 2010, 38, 811-819.
11. Tschoppe P., Zandim D.L., Martus P., Enamel and dentine remineralization by nano-hydroxyapatite toothpastes, *J. Dent.*, 2011, 39, 430-437.
12. Labella R., Braden M., Deb S., Novel hydroxyapatite-based dental composite, *Biomat.*, 1994, 15, 1197-1200.
13. Koutsopoulos S., Synthesis and characterization of hydroxyapatite crystals: a review study on the analytical methods, *J. Biomed. Mat. Res.*, 2002, 62, 600-612.
14. Dorozhkin S.V., Nanodimensional and nanocrystalline calcium orthophosphates, *Int. J. Chem. Mat. Sci.*, 2013, 1, 105-174.
15. Padmanabhana S., Balakrishnana A., Chu M., Sol-gel synthesis and characterization of hydroxyapatite nanorods. *Particuology*, 2009, 7, 466-470.
16. Bilton Q.M., Wallace R., Brydson R., Sol-gel synthesis and TEM-EDX characterization of hydroxyapatite nanoscale powders modified by Mg, Sr or Ti, *J. Phys.: Conference Series*, 2010, 241, 012-042.
17. Agrawal K., Singh G., Puri D., Synthesis and characterization of hydroxyapatite powder by sol-gel method for biomedical application. *J. Min. Mat. Char. Eng.*, 2011, 10, 727-734.
18. Sadat-Shojai M., Khorasani M.T., Dinpanah-Khoshdargi E., Synthesis methods for nanosized hydroxyapatite with diverse structures, *Acta Biomater.*, 2013, 9, 591-621.
19. Taher N.M., Degree of conversion and surface hardness of two nano-composites compared to three other tooth-colored restorative materials, *Pak. Oral Dent. J.* 2011, 31, 457-463.
20. Kaygili O., Dorozhkin S., Keser S., Synthesis and characterization of Ce-substituted hydroxyapatite by sol-gel method, *Mat. Sci. En.*, 2014, 42, 78-82.
21. Hanna A.A., Sherief M.A., Aboelenin R.M., Preparation and characterizations of barium hydroxyapatite as ion exchanger, *C.J.P.A.S.*, 2010, 4, 1087-1093.
22. Yasukawa A., Nakajima M., Kandori K., Preparation and characterization of carbonated barium hydroxyapatites, *J.C.I.S.*, 1999, 212, 220-227.
23. Arcís R.W., López-Macipe A., Toledano M., Mechanical properties of visible light-cured resins reinforced with hydroxyapatite for dental restoration, *Dent. Mat.*, 2002, 18, 49-57.
24. Galvão M.R., Caldas S.G., Bagnato V.S., Evaluation of degree of conversion and hardness of dental composites photo-activated with different light guide tips, *Eur. J. Dent.*, 2013, 7, 86-93.
25. Fleming G., Awan M., Cooper P., The potential of a resin-composite to be cured to a 4 mm depth, *Dent. Mat.*, 2008, 24, 522-529.
26. Flury S., Hayoz S., Peutzfeldt A., Depth of cure of resin composites: Is the ISO 4049 method suitable for bulk fill materials?, *Dent. Mat.*, 2012, 28, 521-528.
27. Roberts H., Berzins D., Charlton D., Hardness of three resin-modified glass ionomer restorative materials as a function of depth and time, *J. Esth. Rest. Dent.*, 2009, 21, 262-274
28. Bhalla M., Patel D., Shashikiran N.D., Effect of light- emitting diode and halogen light curing on the micro-hardness of dental composite and resin-modified glass ionomer cement: An in vitro study *J. Ind. Soc. Ped. Prev. Dent.*, 2012, 30, 201-205.
29. Yap A.U. and Teoh S.H., Comparison of flexural properties of composite restoratives using the ISO and mini-flexural tests, *J. Oral. Rehab.*, 2003, 30, 171-177.
30. Leitune V.C., Collares F.M., Trommer R.M., The addition of nanostructured hydroxyapatite to an experimental adhesive resin, *J. Dent.*, 2013, 41, 321-327.
31. Yoshida K. and Greener E., Effect of two amine reducing agents on the degree of conversion and physical properties of an unfilled light-cured resin, *Dent. Mat.*, 1993, 9, 246-251.
32. Filho J.D., Brandão N.L., Poskus L.T., A critical analysis of the degree of conversion of resin-based luting cements, *J. App. Oral. Sci.*, 2010, 18, 442-446.
33. Sanosh K.P., Avinash B., Min-Cheol C., Sol-gel synthesis and characterization of hydroxyapatite nanorods, *Particuology*, 2009, 7, 466-470.
34. Cheng H., Yasukawa A., Kandori A., FTIR Study of Adsorption of CO₂ on stoichiometric calcium hydroxyapatite, *Langmuir.*, 1998, 14, 6681-6686.
35. Cengiz B., Gokce Y., Yildiz N., Synthesis and characterization of hydroxyapatite nanoparticles, *Phys. Chem. Eng. Asp.*, 2008, 322, 29-33.

36. Anee T.K., Ashok M., Palanichany M., A novel technique to synthesize hydroxyapatite at low temperature, *Mat. Chem. Phys.*, 2003, 80, 725-730.
37. Chen L., Yu Q., Wang Y., Bis-GMA/TEGDMA dental composite containing high aspect-ratio hydroxyapatite nanofibers, *Dent. Mat.*, 2011, 27, 1187-1195.
38. Prasanna N., Pallavi Y., Kavitha S., Degree of conversion and residual stress of preheated and room-temperature composites, *Ind. J. Dent. Res.*, 2007, 18, 173-176.
39. Krämer N., Lohbauer U., García-Godoy F., Light curing of resin-based composites in the LED era, *Am. J. Dent.*, 2008, 21, 135-144.
40. Shortall A.C., Palin W.M, Burtscher P., Refractive index mismatch and monomer reactivity influence composite curing depth, *J. Dent. Res.*, 2008, 87, 84-88.
41. Musanje L. and Darvell B.W., Curing-light attenuation in filled resin restorative materials, *Dent. Mat.*, 2006, 22, 804-817.

***** *****